

This article was downloaded by:

On: 23 January 2011

Access details: *Access Details: Free Access*

Publisher *Taylor & Francis*

Informa Ltd Registered in England and Wales Registered Number: 1072954 Registered office: Mortimer House, 37-41 Mortimer Street, London W1T 3JH, UK



Journal of Carbohydrate Chemistry

Publication details, including instructions for authors and subscription information:

<http://www.informaworld.com/smpp/title~content=t713617200>

2-Dimensional NMR in Carbohydrate Structural Analysis

Steven L. Patt; Varian Associates

To cite this Article Patt, Steven L. and Associates, Varian(1984) '2-Dimensional NMR in Carbohydrate Structural Analysis', Journal of Carbohydrate Chemistry, 3: 4, 493 – 511

To link to this Article: DOI: 10.1080/07328308408057914

URL: <http://dx.doi.org/10.1080/07328308408057914>

PLEASE SCROLL DOWN FOR ARTICLE

Full terms and conditions of use: <http://www.informaworld.com/terms-and-conditions-of-access.pdf>

This article may be used for research, teaching and private study purposes. Any substantial or systematic reproduction, re-distribution, re-selling, loan or sub-licensing, systematic supply or distribution in any form to anyone is expressly forbidden.

The publisher does not give any warranty express or implied or make any representation that the contents will be complete or accurate or up to date. The accuracy of any instructions, formulae and drug doses should be independently verified with primary sources. The publisher shall not be liable for any loss, actions, claims, proceedings, demand or costs or damages whatsoever or howsoever caused arising directly or indirectly in connection with or arising out of the use of this material.

REVIEW ARTICLE

2-DIMENSIONAL NMR IN CARBOHYDRATE STRUCTURAL ANALYSIS

Steven L. Patt

Varian Associates
611 Hansen Way
Palo Alto, CA 94303

Received May 28, 1984

ABSTRACT

2-Dimensional FT NMR techniques have greatly expanded the power of NMR to unravel complex chemical structures. Homonuclear 2D J-resolved experiments can be helpful in sorting out complex overlapping coupling patterns, while homonuclear chemical shift correlation experiments can be used to determine the homonuclear coupling networks. Heteronuclear chemical shift correlation experiments can indicate the source of direct or long-range heteronuclear couplings, and hence can be used to relate the proton spectrum to the carbon spectrum. Carbon-carbon connectivity experiments reflect carbon homonuclear couplings, and, while the most insensitive of all the techniques, can be the most powerful in directly revealing the molecular framework. Techniques such as these can be used either individually or in combination to reveal part or all of the structural features of both simple and complex carbohydrates. The general features of 2D experiments are discussed in the context of their application to carbohydrates.

INTRODUCTION

The field of two-dimensional (2D) NMR encompasses literally hundreds of experiments, which collectively have revolutionized the field of NMR in the past decade. While the experiments differ in the specifics of how they are performed and in the type of results that they produce, they are united by a common framework, and it is with that framework that we begin our discussion of 2D NMR.

In a conventional one-dimensional (1D) FT NMR experiment, data are collected as a function of time. These data are called the free induction decay or FID. The oscillations, or frequencies, present in this signal are analyzed by means of a Fourier transformation, which transforms data from the "time domain" into the "frequency domain". That is, after the transformation, we plot the spectrum as a function of frequency, whereas before the transformation we plot (or display) the FID as a function of time.

In many cases it becomes useful to obtain a series of such 1D spectra. For example, we might obtain spectra as a function of decoupling frequency, or as a function of temperature. We might also obtain spectra as a function of time. This time might be "real" time, such as in the observation of reaction kinetics, or it might be a time variable under our control, as part of a pulse sequence.

One of the concepts that gives the technique of FT NMR so much versatility is that of the pulse sequence. Rather than just applying a simple pulsed excitation (i.e., a pulse) and observing the FID, we can apply a pulse, wait for a time, apply another pulse, and then observe the signal. A sequence of pulses and delays, applied in some order, is known as a pulse sequence.

One of the first pulse sequences developed was the inversion-recovery pulse sequence.¹ In this experiment, a 180° pulse is applied which inverts the magnetizations of the spins. After a time commonly known as tau, during which the spins return partially or entirely to their original "right-side-up" orientation (aligned along the magnetic field), a 90° pulse is applied to sample the magnetization. By varying the delay tau and repeating the experiment, we obtain a series of spectra, with the peak height(s) in each spectrum reflecting the (usually) exponential progress of the peak(s) from the inverted state back to the equilibrium state.

Consider a series of such spectra (FIG. 1). To analyze this data, we first measure the peak heights in the spectra and then plot these as a function of the time tau (FIG. 2). In the case of an exponential process such as this one, the usual tool of analysis is a computer curve fitting program.

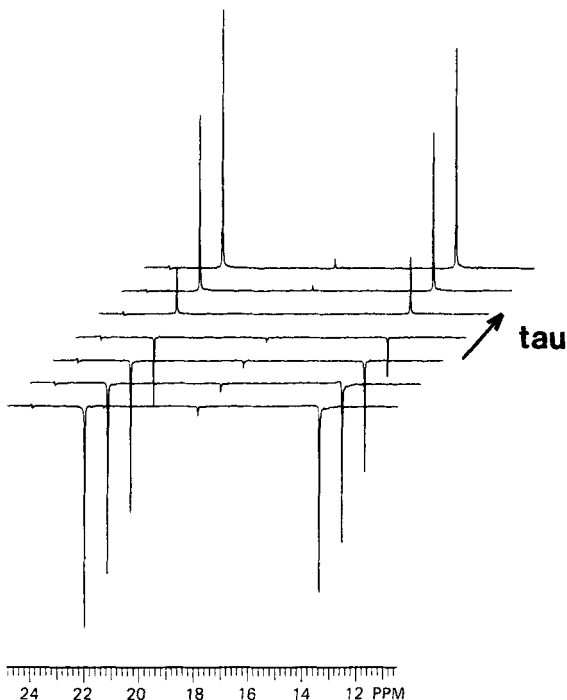


Figure 1. ^{13}C inversion-recovery T_1 experiment of a sample of 3-Heptanone. The pulse sequence used is $D1-180^\circ\text{-tau-}90^\circ\text{-acquire}$, with $\tau = 0.375, 0.75, 1.5, 3.0, 6.0, 12.0,$ and 24.0 seconds from bottom to top, and $D1=24.0$ sec. Only part of each spectrum is plotted.

Pulse sequences have grown in complexity since the introduction of the inversion-recovery sequence. 2D experiments are a particular class of pulse sequences, whose common characteristic is this: if we obtain a series of spectra as a function of τ , and then plot the height of any peak as a function of τ , that height will vary not exponentially but sinusoidally. That is, the peak height will oscillate (and decay) as a function of τ .

Many 1D NMR experiments in common use, including APT,² INEPT,³ and DEPT,⁴ actually belong to the same class of pulse sequences but are commonly performed using only a small number (one to three) of τ values to reveal carbon multiplicity informa-

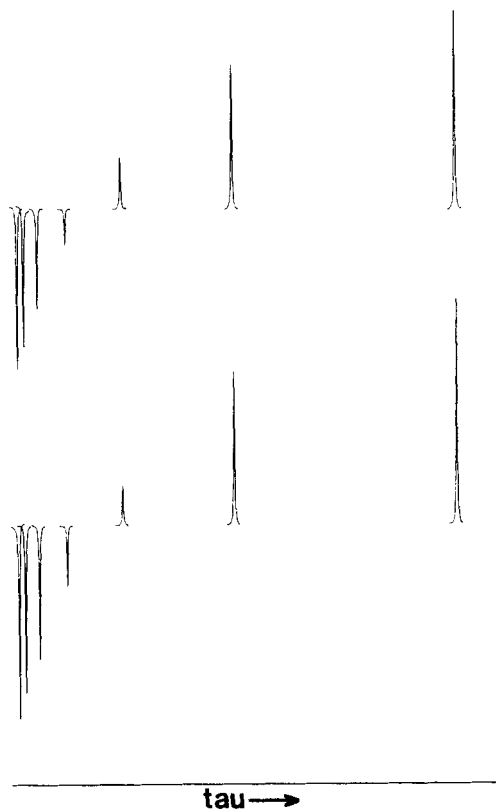


Figure 2. T_1 plot of the peaks extracted from FIG. 1, showing the two peaks at 13.4 ppm (top) and 22.0 ppm (bottom). The peaks have been plotted with an x-coordinate proportional to the value of tau, so that the plots exhibit directly the exponential behavior of the peak heights as a function of tau.

tion. In a conventional APT experiment, for example, we obtain a spectrum at a single tau value (commonly 7 or 8 msec). In such a spectrum, we can identify methylene and quaternary carbons by their positive amplitude, methyl and methine carbons by their negative amplitude. Distinguishing between methyls and methines, or methylenes and quaternaries, cannot be done on the basis of a single spectrum.

If we perform not a single APT experiment, however, but a whole series of such experiments, we obtain the results shown in FIG. 3. The oscillation of the peak heights as a function of tau is clearly in evidence. If we extract the peak heights from each of these spectra, and plot them as a function of tau, we obtain the results seen in FIG. 4. A plot such as this, which oscillates as a function of time, is known as an interferogram.

The oscillatory behavior thus observed can be analyzed to determine the frequency or frequencies of oscillation. Any number of computer programs could accomplish this task, but there is one which is by far the most efficient - Fourier transformation, whose sole purpose is to analyze oscillating signals. The right half of FIG. 4 shows the results of such a Fourier transformation, in which the frequencies of oscillation have now become explicit. The peak at 13.4 ppm reveals itself to be a quartet (and hence a methyl carbon), the peak at 22.0 ppm a triplet (and hence a methylene).

We have discussed and illustrated this process merely as a question of extracting the peak heights of selected resonances as a function of time, and in fact this can be done. Often, however, it is simpler to treat the entire original data set in this manner. That is, we form the first interferogram out of the first data point from each of our original spectra, the second interferogram from the second data point of each of the original spectra, etc. This process is nothing more than the mathematical process of matrix transposition. After Fourier transformation of each of these interferograms, we obtain a plot of intensity vs. frequency in two dimensions. FIG. 5 shows the results of this complete process, where the data has been plotted both in the form of a series of individual spectra (stacked or "white-washed" plot), as well as in the form of a contour plot, in which each successive contour represents a higher intensity.

Since we start with a series of "normal" spectra (normal with respect to the frequencies of the observed resonances if not with respect to their intensities), it is clear that one axis of any 2D plot will be our normal spectral axis, that is, a conventional 1D spectrum of the sample can always be lined up on one

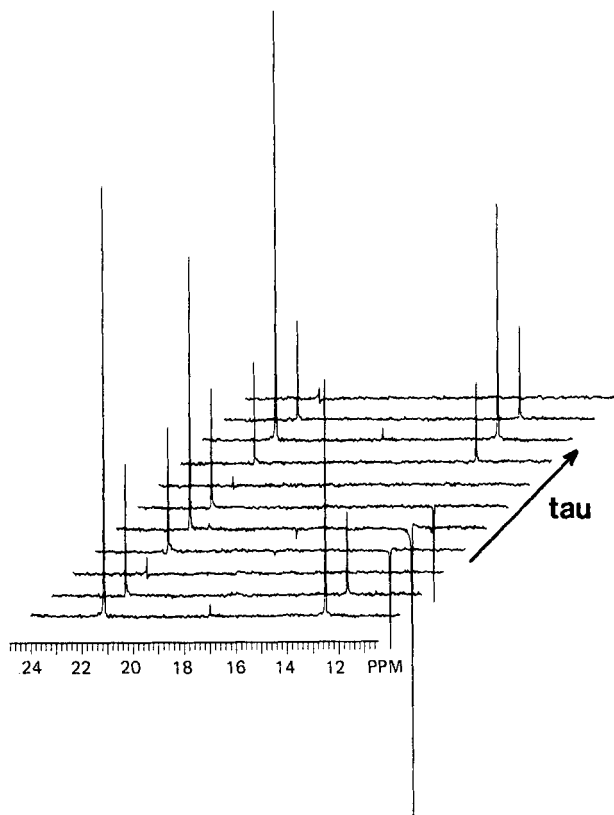


Figure 3. A series of ^{13}C APT spectra of 3-Heptanone. The pulse sequence used is $D1-90^\circ-\tau-180^\circ-\tau-D3-180^\circ-D3$ -acquire, with $D1=0$, $D3=1$ msec, and τ varying from 0 to 20 msec in steps of 2 msec from bottom to top. The proton decoupler is on at all times except during the first τ delay. Only part of each spectrum is plotted.

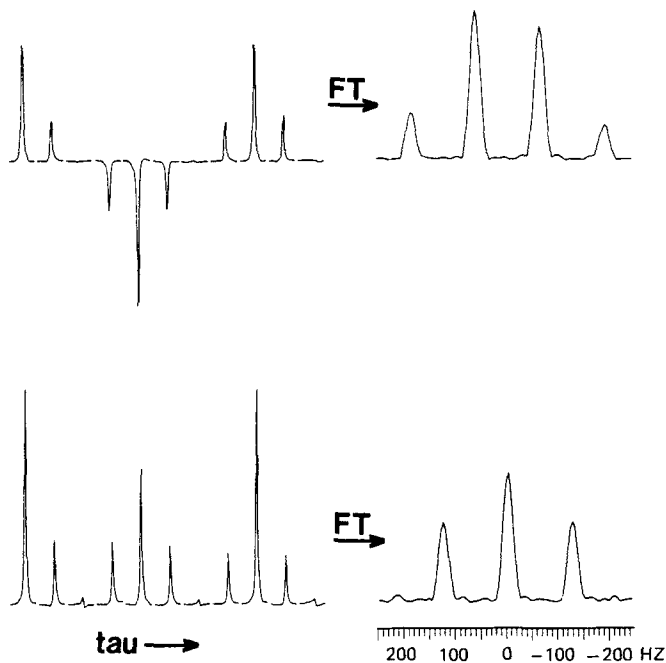


Figure 4. A plot of the peaks extracted from FIG. 3, showing the two peaks at 13.4 ppm (upper left) and 22.0 ppm (lower left). The peaks have been plotted with an x-coordinate proportional to the tau value, so that the plots directly exhibit the oscillatory behavior of the peak height as a function of tau. After Fourier transformation of a larger number (64) of such experiments (upper and lower right), the oscillation frequencies are plotted directly, on a scale of ± 250 Hz.

axis of any 2D plot. It is this axis which represents the signals actually detected in the receiver of the spectrometer during a time conventionally labelled t_2 , and hence this axis becomes the f_2 axis. The second axis (or "domain"), known as the f_1 axis, is the axis along which the frequencies of oscillation of our original peaks will appear following the second Fourier transformation. This axis can contain a variety of information, depending on the particular experiment chosen, that is, depending on which pulse sequence is employed. In the 2D APT or Heteronuclear 2D

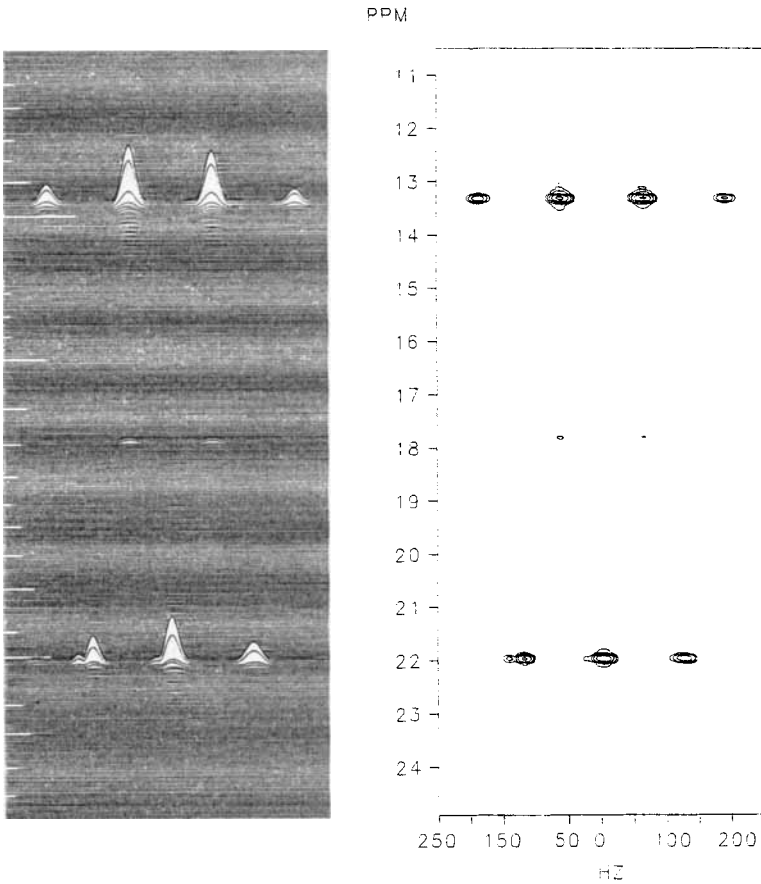


Figure 5. Full two-dimensional transform of the data from FIG. 3. On the left, the data are in the form of a "white-washed" plot, in which each spectrum is the result of Fourier transformation of a single interferogram. On the right, the same data is plotted in the form of a contour plot. Each successive contour line represents an increase in intensity by a factor of two.

J-resolved experiment⁵ illustrated in FIG. 5, this axis contains heteronuclear J-couplings.

2D pulse sequences consist of one or more pulses and delays preceding the final observation of the signal. Typically, all but one of the delays will be fixed; one, which we have called tau but in 2D experiments is commonly denoted t_1 , will be varied to cause the peak height oscillation we will observe during t_2 . The time t_1 is also commonly known as the evolution time, since it is the evolution of the nuclear magnetizations during this period which is later indirectly detected in the signal measured during t_2 .

As a consequence of the fact that the analysis of the data as a function of t_1 will be done using a Fourier transform, the data must be obtained using regularly spaced values of t_1 (in contrast to the inversion-recovery experiment where non-linear spacing of t_1 values is both permissible and customary). As required by the Nyquist theorem, if the frequencies to be detected cover a range $\Delta\nu$, then the experiment must be repeated with intervals (or increments) of $t_1 = 1/\Delta\nu$. If we perform a number of experiments (increments) which we call NI, then the longest value of the evolution time is $NI/\Delta\nu$, and the resolution in the f_1 domain is $\Delta\nu/NI$. Thus the resolution is inversely proportional to the experiment time, in exactly the same way that the limiting resolution in the f_2 domain is inversely proportional to the data acquisition time (AT) for each FID. For ^1H spectra in particular, we will often find that the resolution rather than the sensitivity determines the time necessary for the experiment.

While there are hundreds of 2D pulse sequence variations, a few common types emerge. One, illustrated above, is the J-resolved 2D experiment. In such experiments the second frequency domain contains coupling constants, be they homo- or heteronuclear, direct or long-range.

Another major class of experiments is chemical shift correlation, in which we plot in the second domain the chemical shift of a nucleus which is coupled to the observed nucleus. Such couplings can again be homo- or heteronuclear, direct or long-range, or even indirect (relayed via a third nucleus).

A third class of experiments involves magnetization transfer between nuclei as reflected in such properties as NOE and chemical exchange. 2D-NOE experiments in particular can detect the through-space interactions which can be a valuable complement to the through-bond interactions determined in the chemical shift correlation experiment.

The final class of experiments is that in which the frequencies detected during t_1 are themselves not directly detectable, that is, multiple quantum transitions. The most widely used of this class of experiments is the powerful carbon-carbon connectivity experiment, with which carbon-carbon bonds can be determined.

RESULTS AND DISCUSSION

Conventional 1D ^1H NMR spectra are complicated by the fact that both chemical shift and coupling information appear on the same axis. The homonuclear J-resolved 2D experiment⁶ enables us to resolve this problem, by detecting in the f_1 domain coupling information only (for the details of this and other pulse sequences described here the reader is referred to the appropriate references). FIG. 6 shows such a spectrum for methyl β -D-glucopyranoside. Starting from the downfield side of the spectrum, the first two peaks show f_1 frequencies of approximately + and - 4 Hz, respectively. This frequency is precisely the difference frequency between the peak in question and the chemical shift of the multiplet to which it belongs. Since we detect one positive and one negative f_1 frequency, we know immediately that these two peaks form a doublet. Since the separation of these two peaks along the f_1 axis is precisely the separation along the f_2 axis, the peaks in the 2D spectrum fall on a straight line, whose angle is 45° in frequency space (that is, 45° if we plot the spectrum with an equal number of Hz/cm along both axes).

In a like manner we can identify many of the resonances in the spectrum as belonging to a single multiplet. The four peaks between 3.8 and 3.9 ppm form a straight line, as do the four between 3.6 and 3.7 ppm. We can likewise identify doublets of doublets centered at 3.45 ppm, 3.3 ppm, and 3.2 ppm. The intense $-\text{OCH}_3$ peak at 3.5 ppm (off-scale in the 1D plot) gives

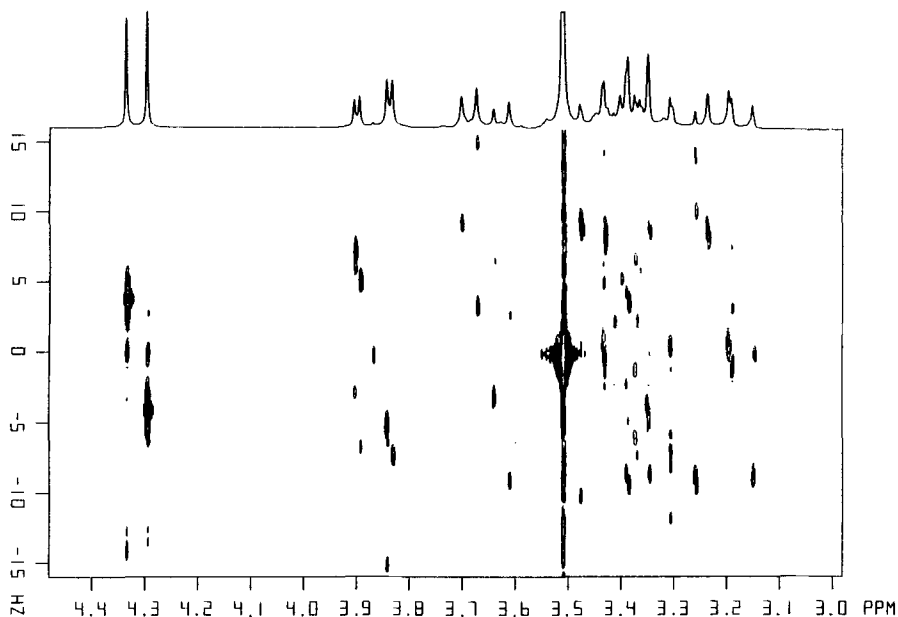


Figure 6. Homonuclear J-resolved spectrum of methyl β -D-glucopyranoside in D_2O . The spectrum along the top is a 1D proton spectrum of the same sample.

a peak at 0 Hz along the f_1 axis, since it is not coupled. It also shows a long "tail" in the f_1 axis, which is much less intense than the peak but more intense than the resonances from the remaining protons. We have thus accounted for, although not assigned, all but one of the protons in the molecule. Clearly, the remaining proton falls between 3.3 and 3.5 ppm, but its exact location is not yet clear.

In our 2D spectrum we observe, in addition to the peaks of interest, a number of other peaks. Virtually all of these are "real", but they complicate the analysis. We can simplify matters, however, by performing a mathematical rotation of the data by 45° in frequency space, so that the multiplets "line up", as seen in FIG. 7. If we now remove any spectral features which do not appear symmetrically on both sides of the $J=0$ axis, we remove the great majority of the uninteresting peaks, as well as the tail

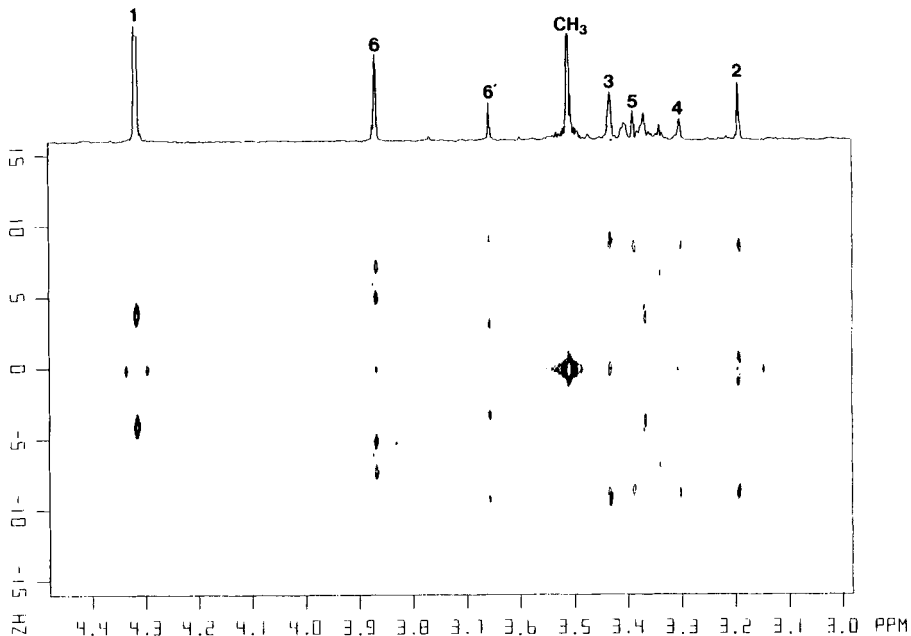


Figure 7. The data of FIG. 6 after rotation by 45° in frequency space and symmetrization about the $J=0$ axis. The spectrum along the top is a projection of the 2D data onto the f_2 axis.

of the large $-\text{OCH}_3$ peak. Since the coupling information is now exclusively along the f_1 axis, a projection of the data onto the f_2 axis gives a spectrum which reflects only chemical shifts, and is effectively a "broadband proton decoupled" ^1H spectrum.

The analysis of the region between 3.3 and 3.5 ppm is complicated by second-order effects.⁷ From the homonuclear chemical shift correlation experiment⁸ (*vide infra*), we will arrive at the assignments which are marked on the projection. Two of the three spurious resonances in the projected spectrum can then be accounted for, as we find one halfway between H-3 and H-4, and another halfway between H-4 and H-5, which is expected for strongly coupled multiplets.⁷

Having at least a reasonable idea of how many protons there are and where they fall in the spectrum, we now obtain a homonuclear chemical shift correlation spectrum (FIG. 8). In this experiment, the f_1 axis reflects the frequencies of all peaks coupled to the observed peaks. Since each peak is "coupled" to itself, we observe first of all a series of resonances along the diagonal, that is, peaks for which $f_1=f_2$. The peaks in the upper left of the spectrum represent such information. The six peaks in the upper right of the spectrum, however, indicate real coupling, namely, that the doublet at 4.3 ppm is coupled to the triplet (doublet of doublets) at 3.2 ppm. Thus if the doublet at 4.3 ppm is H-1, the peaks at 3.2 ppm must be H-2, and we can continue in this vein to assign all of the protons in the spectrum.

A useful way to do this is to project sections of the data, as shown by the dotted lines, onto the f_1 axis (FIG. 9). FIG. 9b represents H-1 and all protons coupled to H-1, thus identifying H-2. FIG. 9c represents H-2 and all protons coupled to it, identifying H-3. Only one of the lines of H-3 does not overlap other resonances, so we take this line and project section d, which then shows us H-3 and all protons coupled to it. We also see in FIG. 9d a peak from the nearby intense $-\text{OCH}_3$ resonance, which clearly represents overlap and not coupling. Finally, FIG. 9e represents H6 and the protons coupled to it, H-6' and H-5. From FIGS. 9c and e we can then read the frequencies of H-3 and H-5 as 3.43 and 3.38 ppm, respectively, which agrees extremely well with the frequencies seen in the homonuclear J-resolved experiment (FIG. 7).

With the assignment of the ^1H spectrum now in hand, we proceed to a heteronuclear chemical shift correlation experiment⁹ (FIG. 10), in which we detect ^{13}C signals during t_2 and measure along the f_1 axis the spectrum of the protons attached to each carbon. By plotting slices from such a spectrum (FIG. 11), we can actually plot one by one the spectrum of each proton in the molecule, having separated them not by using higher magnetic fields but by using instead the greater resolving power of the ^{13}C spectrum. The ^1H frequencies observed in this series of spectra agree

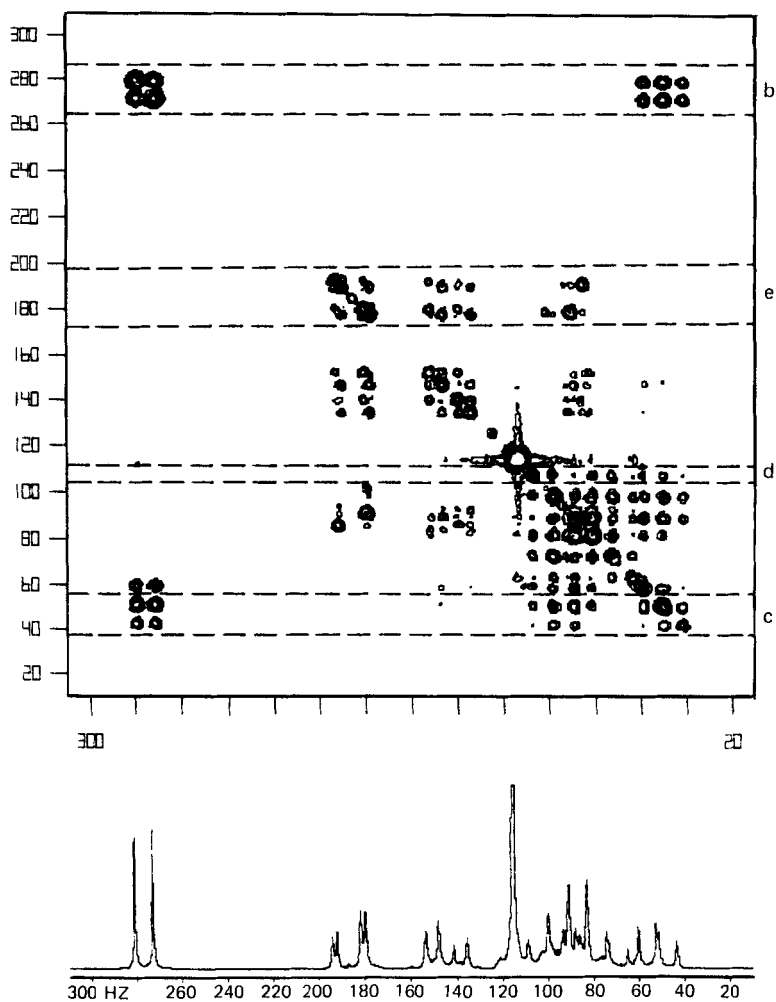


Figure 8. Homonuclear chemical shift correlation spectrum of methyl β -D-glucopyranoside in D_2O . The spectrum along the bottom is a 1D proton spectrum of the same sample. The sections of the data between the dotted lines will be referred to below.

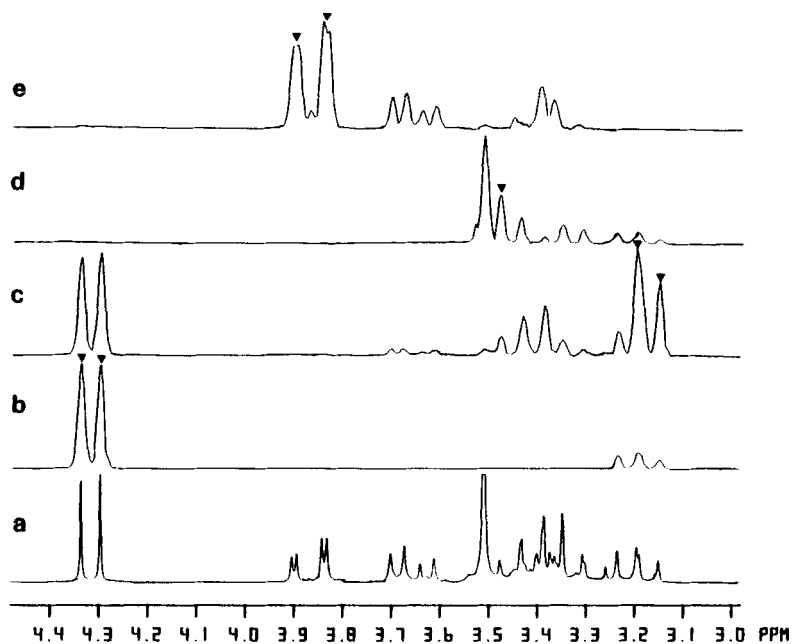


Figure 9. a) 1D proton spectrum of methyl β -D-glucopyranoside in D_2O . b) A projection of the data from FIG. 8 onto the f_2 axis, taken between 4.25 and 4.35 ppm, as indicated in FIG. 8. The peaks marked with an arrow are the peaks whose coupling is detected by this projection. c) A projection of the data from 3.1 to 3.2 ppm. d) A projection of the data near 3.48 ppm. e) A projection of the data between 3.8 and 3.95 ppm.

exactly with those measured in either the homonuclear J-resolved or the homonuclear chemical shift correlation experiments, as they should. Since we have assigned the proton spectrum, this series of spectra enables us then to assign the ^{13}C spectrum.

As molecular complexity increases, it is not always possible to completely assign the 1H spectrum from the homonuclear J-resolved and chemical shift correlation experiments. If we could assign the ^{13}C spectrum first, however, we could then use the heteronuclear chemical shift correlation experiment to interpret the 1H

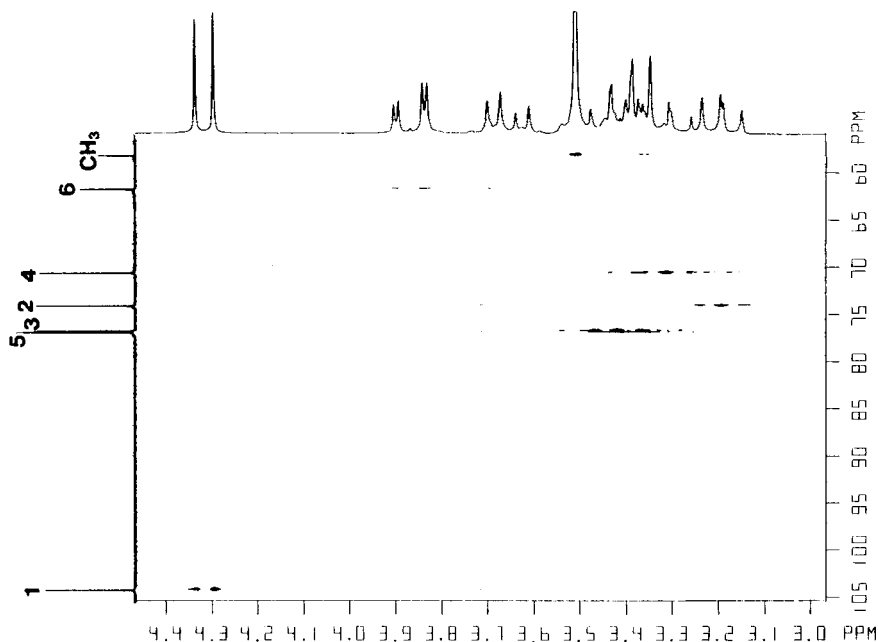


Figure 10. Heteronuclear chemical shift correlation spectrum of methyl β -D-glucopyranoside in D_2O . The spectrum along the top is a 1D proton spectrum of the same sample, the spectrum along the left side is the 1D carbon spectrum.

spectrum, essentially reversing the method used above. A sample of glucose in D_2O provides a 1H spectrum complicated enough to require this approach.

The experiment that we use to assign the ^{13}C spectrum is known as 2D INADEQUATE,¹⁰ or carbon-carbon connectivity. In this experiment, we indirectly detect during t_1 a phenomenon known as double-quantum coherence which can be generated in molecules with ^{13}C - ^{13}C coupling. Since such coupling is only detected in molecules with two adjacent ^{13}C nuclei, the sensitivity of this experiment is extremely weak (without ^{13}C enrichment). The results, however, can be most gratifying.

In FIG. 12 we see a carbon-carbon connectivity plot (CCCP) for a sample of mutarotated glucose in D_2O . The f_2 axis, here

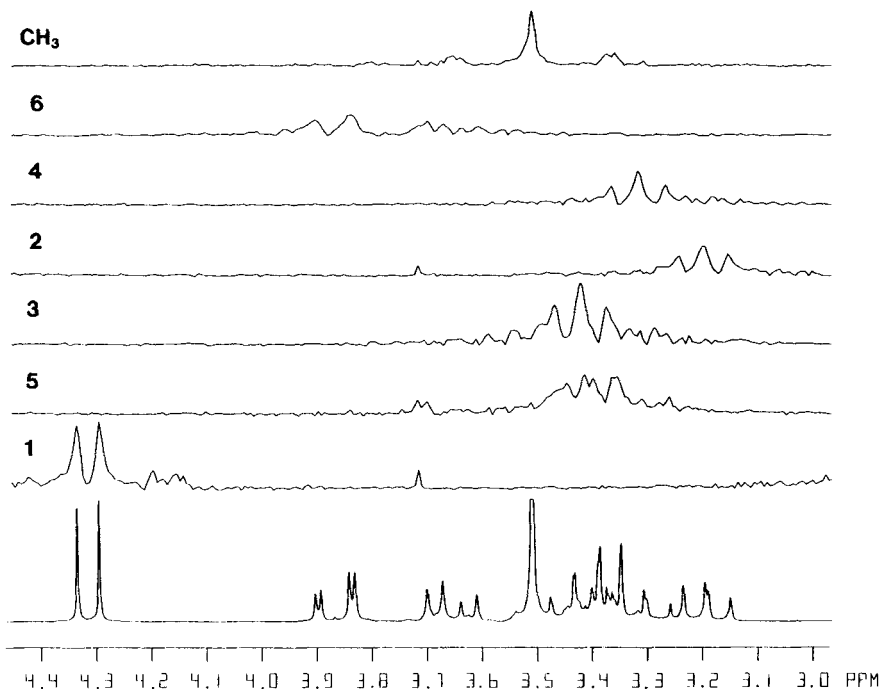


Figure 11. Individual spectra extracted from FIG. 10, each showing the spectrum of proton(s) attached to a single carbon atom, as labelled.

plotted horizontally, shows ^{13}C chemical shifts, but all isolated ^{13}C resonances are suppressed, leaving only ^{13}C - ^{13}C doublets. For each carbon we detect as many such doublets as there are other carbons bonded to that carbon. The displacement along the y-axis, which is the double quantum frequency, is the same for carbons bonded to each other, and hence a carbon-carbon bond is represented simply by a horizontal line connecting pairs of doublets, as seen in FIG. 12 for the C-1 to C-2 bond in β -D-glucopyranose. Simply by finding all such pairs of doublets we can completely assign the ^{13}C spectrum, as indicated in FIG. 12b, with absolutely no interpretation required. Parenthetically, this experiment reverses the assignment of C-4 α and C-4 β found in Pfeffer *et al.*¹¹

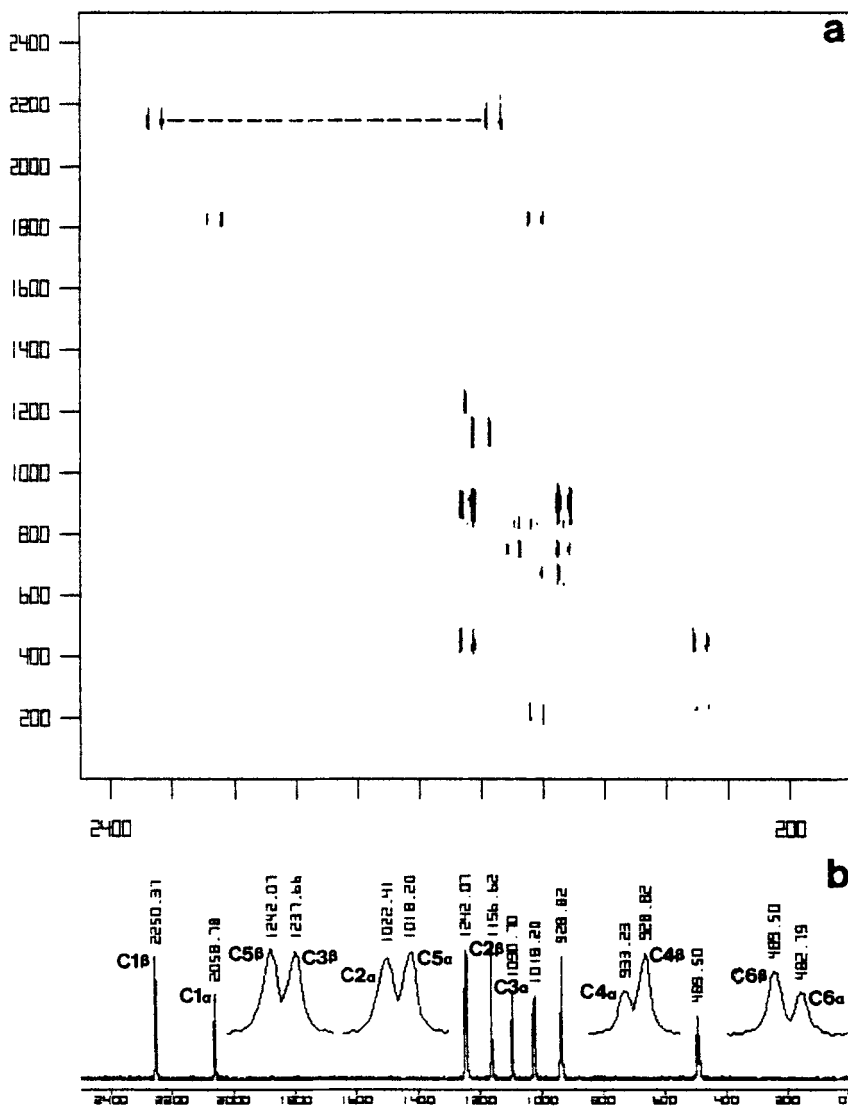


Figure 12. a) Carbon-carbon connectivity plot for an equilibrium mixture of glucose in D_2O , with the detection of the bond between C-1 and C_2 in β -D-glucopyranose indicated by the dotted line. ^{13}C chemical shift is plotted horizontally, and double quantum frequency plotted vertically. b) 1D ^{13}C spectrum showing the assignment of all carbon resonances, including all four closely spaced pairs of lines.

EXPERIMENTAL

All 2D experiments presented in the INTRODUCTION were performed on a Varian XL-300 spectrometer. 3-Heptanone (Aldrich) was run as a 30% (volume) solution in CDCl_3 (Stohler Isotope). Experiments presented in the RESULTS AND DISCUSSION section were performed on a Varian XL-200 spectrometer. Methyl β -D-glucopyranoside (Sigma) was run as a 50 mg/ml solution in D_2O (Merck Sharp & Dohme). β -D-glucopyranose (Calbiochem) was run as a 500 mg/ml solution in D_2O . All data acquisition and processing were performed with standard Varian software.

REFERENCES

1. R. L. Vold, J. S. Waugh, M. P. Klein, and D. E. Phelps, J. Chem. Phys., **48**, 3831 (1968).
2. S. L. Patt and J. N. Shoolery, J. Magn. Reson., **46**, 535 (1982).
3. D. P. Burum and R. R. Ernst, J. Magn. Reson., **39**, 163 (1980).
4. D. M. Doddrell, D. T. Pegg, and M. R. Bendall, J. Magn. Reson., **48**, 323 (1982).
5. G. Bodenhausen, R. Freeman, and D. L. Turner, J. Chem. Phys., **65**, 839 (1976).
6. W. P. Aue, J. Karhan, and R. R. Ernst, J. Chem. Phys., **64**, 4226 (1976).
7. G. Bodenhausen, R. Freeman, G. A. Morris, and D. L. Turner, J. Magn. Reson., **31**, 75 (1978).
8. A. Bax, R. Freeman, and G. A. Morris, J. Magn. Reson., **42**, 169 (1981).
9. A. Bax and G. A. Morris, J. Magn. Reson., **42**, 501 (1981).
10. A. Bax, R. Freeman, T. Frenkiel, and M. H. Levitt, J. Magn. Reson., **43**, 478 (1981).
11. P. E. Pfeffer, K. M. Valentine, and F. W. Parrish, J. Amer. Chem. Soc., **101**, 1265 (1979).